Spiralling in BTA deep-hole drilling – Models of varying frequencies

Nils Raabe Oliver Webber Winfried Theis
Claus Weihs

September 30, 2005

Abstract

One serious problem in deep-hole drilling is the formation of a dynamic disturbance called spiralling which causes holes with several lobes. Since such lobes are a severe impairment of the bore hole the formation of spiralling has to be prevented. Gessesse et al. (1994) explain spiralling by the coincidence of bending modes and multiples of the rotary frequency. They derive this from an elaborate finite elements model of the process.

In online measurements we detected slowly changing frequency patterns similar to those calculated by Gessesse et al. We therefore propose a method to estimate the parameters determining the change of frequencies over time from spectrogram data. This allows to simplify significantly the usage of the explanation of spiralling in practice because the finite elements model has to be correctly modified for each machine and tool assembly while the statistical method uses observable measurements. Estimating the variation of the frequencies as good as possible opens up the opportunity to prevent spiralling by e.g. changing the rotary frequency.

1 Introduction

The work presented in this paper has been carried out as part of a project aimed at modelling the BTA deep hole drilling process, with special emphasis on dynamic aspects. The longterm goal is online-prediction of dynamic

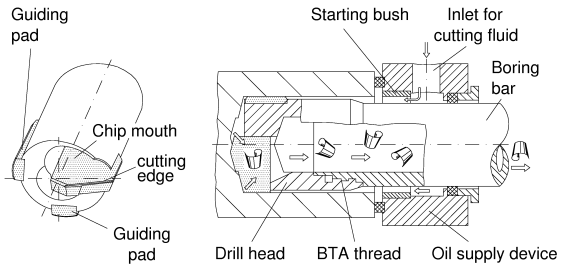

Figure 1: BTA deep hole drilling, working principle (VDI,1974).

disturbances which in future may be used as a basis for intelligent control of the process.

Deep hole drilling methods are used for producing holes with a high length-to-diameter ratio, good surface finish and straightness. For drilling holes with a diameter of 20 mm and above, the BTA (Boring and Trepanning Association) deep hole machining principle is usually employed (see VDI, 1974). The working principle is illustrated in Fig. 1.

For obtaining a low deviation of the bore hole center axis from the ideal straight line, which is an important objective for machining holes with a high length to diameter ratio, deep hole drilling tools use the bore hole wall section machined in the immediate past as a guiding surface. This is achieved by an asymmetric cutting edge arrangement in combination with guiding pads on the circumference of the tool. The high surface finish of the bore hole wall is a side effect of the guiding action.

When drilling with standard twist drills, chip removal becomes more and more unreliable with increasing drilling depth. This sooner or later leads to process failure. To solve this problem, deep hole drilling tools feature forced chip removal through high cooling lubricant flow rates via low restriction passages. In the case of BTA deep hole drilling, oil is supplied around the outside of the boring bar and the chips are transported away through the internal volume of the tube.

Machining of bore holes with a high length to diameter ratio necessitates slender tool-boring bar assemblies. These components therefore have low dynamic stiffness properties which in turn can be the cause of dynamic dis-

Figure 2: Radial chatter marks on the bottom of the bore hole (left) and effects of spiralling on the bore hole wall (right).

turbances such as chatter vibration and spiralling. Whereas chatter mainly leads to increased tool wear along with marks on the generally discarded bottom of the bore hole, spiralling causes a multi-lobe shaped deviation of the cross section of the hole from absolute roundness often constituting a significant impairment of the workpiece. The effects of these disturbances on the workpiece can be seen in Fig. 2.

As the deep drilling process is often used during the last production phases of expensive workpieces, process reliability is of prime importance. To achieve an optimal process design with the aim of reducing the risk of workpiece damage, a detailed analysis of the process dynamics is necessary.

In this paper we focus on spiralling which can be observed to occur either reproducibly at a certain drilling depth and fixed machining parameters or at random drilling depths. Gessesse et al. (1994) have modelled the process with finite elements and derived from this model that a reason for the reproducible occurence of spiralling is the intersection of changing bending modes and uneven multiples of the rotational frequency. They have shown in some experiments that this actually was a good prediction of spiralling.

We observed the movement of the bending modes in online measurements of the bending moment of the boring bar and in measurements of the lateral acceleration of the boring bar. In Raabe et al. (2004) we estimated the time-variation of bending eigenfrequencies by quadratic regression of spectrogram data on time. Here we propose a method to estimate the course of the frequencies based on the measurements in the framework of a mechanical model.

This paper continues with a description of the mechanical model in section 2. Then section 3 introduces our criterion for parameter selection before some results are presented in section 4. The paper concludes in a summary given in section 5.

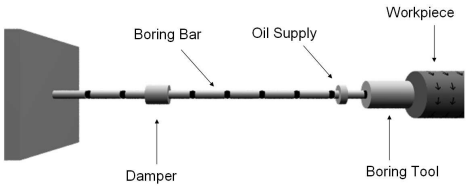

Figure 3: Components of the discretized analogous model.

2 Mechanical Model

To express the connection between the machine parameters and the time-variation of the bending eigenfrequencies (abbreviated BEF) from a mechanical point of view we propose a discretized analogous model (see Gross et al. (2002a)). For this purpose we reduce the BTA system to its most important components (see Fig. 3).

The black dots in fig 3 indicate that for our model we subdivide the bar into n segments – called elements – of equal length $l = L/n$, mass $m = M/n$ and stiffness $k = K \cdot l^2(1, ..., n)'(1, ..., n)$, where L, M and K denote the corresponding values of the whole bar. The number n is called the number of Degrees of Freedom. The stiffness influences of the damper, the oil supply and the workpiece to the boring bar are called k_{supp}, k_{seal} and k_{end}. In contrast to l, m and k the latter three parameters are not known. With these terms the equation of movement of the system can be expressed by:

$$[M]\{\ddot{x}\} + [K]\{x\} = \{0\}$$

with the mass-matrix $[M]_{n\times n} = m \cdot I_{n\times n}$ and the stiffness-matrix

$$[K]_{n\times n} = \frac{k}{l^2} \begin{bmatrix} 6 & -4 & 1 & 0 & \cdots & \cdots & 0 \\ -4 & 6 & -4 & 1 & \ddots & & \vdots \\ 1 & -4 & 6 & \ddots & \ddots & \ddots & \vdots \\ 0 & 1 & \ddots & \ddots & -4 & 1 & 0 \\ \vdots & \ddots & \ddots & -4 & 6 & -4 & 1 \\ \vdots & & \ddots & 1 & -4 & 5 & -2 \\ 0 & \cdots & \cdots & 0 & 1 & -2 & 1 \end{bmatrix}$$

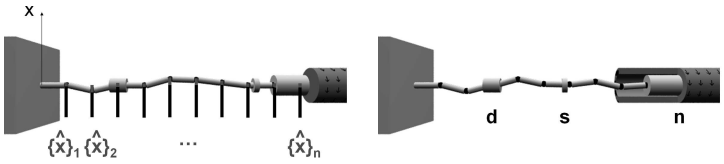

Figure 4: (a) Example of a bending eigenmode. (b) Example of a changing BEM during the drilling process. The position s of the seal changes from value 9 at the beginning (cp. (a)) to 6 while the positions d and n of the influences of damper and workpiece stay the same.

$$+k_{supp}\{e_d\}\{e_d\}' + k_{seal}\{e_s\}\{e_s\}' + k_{end}\{e_n\}\{e_n\}', \tag{1}$$

where d and s represent the numbers of the elements the damper resp. the oil supply device rest on counted from the left. Now determining the BEFs ω and bending eigenmodes (BEMs) $\hat{x}$ of the system means solving the following eigenvalue-problem (compare Gross et al. (2002b)):

$$\left([K] - \omega^2 [M]\right) \{\hat{x}\} e^{i\omega t} = \{0\}. \tag{2}$$

A BEM is the shape with which the bar oscillates with the corresponding BEF. Each BEM is represented by the vector $\hat{x}$ containing the deviations from the baseline in x-direction for each segment end (compare Fig. 4 (a)).

Now the time-variation of the BEMs and BEFs becomes clear when looking at what happens during the drilling process. The boring bar is fixed on the left side and when the process starts the workpiece is rotated and moved towards the bar. While the damper always stays on the same position d the seal of the oil supply moves in front of the workpiece with the same speed (see Fig. 4 (b)). So s decreases and the stiffness matrix $[K]$ changes. Note that even though the workpiece also moves, k_{end} is always added to the nth element of the "base" matrix in the first row of the definition of Eq. 1. This is because the workpiece always affects the end of the bar.

As mentioned above the stiffness parameters k_{supp}, k_{seal} and k_{end} are not known. But in early experiments it turned out that the higher the value is chosen for k_{end} – i.e. the end of the bar nearly can not oscillate – the better is the model fit. So k_{end} from now is fixed to a high value (10^{17}N/m) and the remaining free parameters are k_{supp} and k_{seal}.

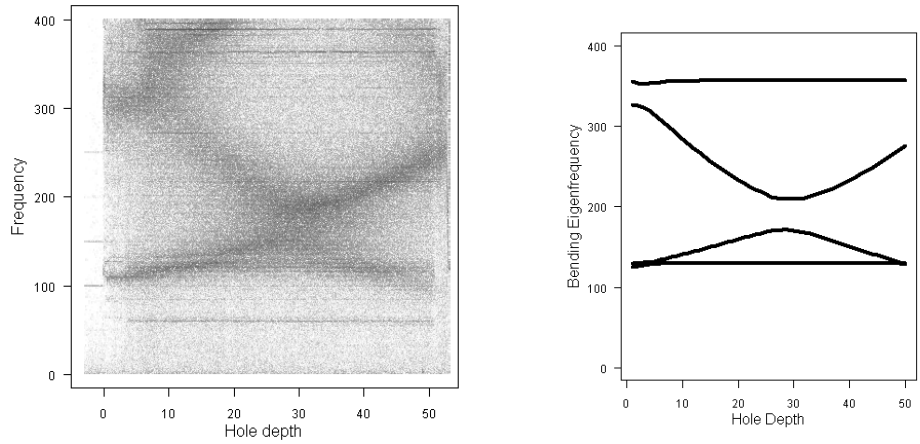

Figure 5: (a) Spectrogram of the acceleration signal. (b) Computed course of bending eigenfrequencies.

3 Criterion

In this section we describe how the two free parameters are estimated. For the fitting we use the data obtained from the acceleration sensor. This sensor is placed between the damper and the final position of the seal. For this reason we except only those BEFs to be prominent in this signal whose corresponding BEMs have a bulge at this position. Computing BEFs and BEMs for a variety of plausible stiffness parameters it shows that these are the second and the third BEF where by definition the lowest BEF is the first one. However, higher BEFs are neglected since the corresponding amplitudes decrease w.r.t. higher frequencies.

Figure 5 (a) shows the spectrogram of the acceleration signal of one of our experiments. Comparing it to a course of the first four BEFs (Fig. 5 (b)) computed by solving Eq. 2 with $L = 334\text{cm}$ and $M = 26\text{kg}$ (known from our settings), some example parameters $k_{supp} = 3.51 \cdot 10^9 \text{N/m}$ and $k_{seal} = 1.053 \cdot 10^7 \text{N/m}$ and $n = 334$ some similarities can be seen. So we recognize the (mirrored) U-Shape of the third (second) BEF.

We also see that the first and fourth computed BEFs nearly don't change. Looking at the corresponding BEMs one would see that they have a bulge between damper and clamped end. Because the damper is expected to have a quite high stiffness, moving the seal does not affect this mode. On the other hand the bar nearly doesn't oscillate in the area where the signal is measured

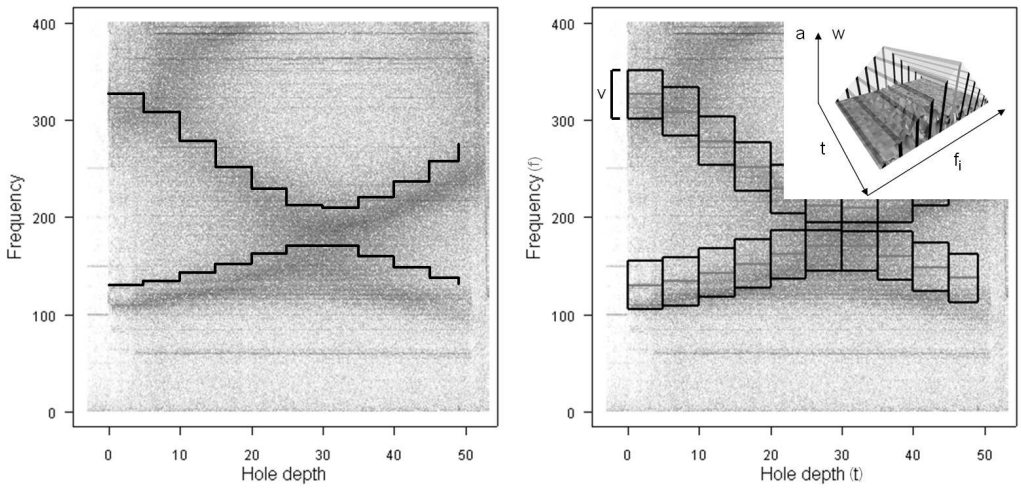

Figure 6: (a) Spectrogram with computed bending eigenfrequencies
(b) Weighting scheme, notice the bandwidth v

with these two frequencies. So they are not reflected in the spectrogram.

However, in the spectrogram there seem to exist some time-constant frequencies with high amplitudes, for example one at about $60Hz$. But for the given reasons we don't assume them to reflect BEFs. It is more plausible that they are due to the machine drive and so are negligible for our investigations.

So our choice of a criterion for any given $\hat{k}_{supp}$ and $\hat{k}_{seal}$ is based on the concordance of the course of the resulting second and third BEF and the spectrogram. Its construction is described in the following.

Let $\hat{\omega}_j(t) := \omega_j(t; \hat{k}_{supp}, \hat{k}_{seal}), j = 2, 3$, be the two interesting BEF courses. Remember these courses are stepfunctions (cp. Fig. 6 (a), for better illustration with a smaller value of n).

Let now

$$f_{c_j}(t), c_j := argmin_i \left(|f_i - \hat{\omega}_j(t)| \right), j = 2, 3,$$

be the Fourier frequencies next to the computed BEFs at each time.

Then the criterion to be maximized is

$$m\left(\hat{k}_{supp}, \hat{k}_{seal}\right) := \frac{1}{2} \sum_{j=2}^{3} \frac{1}{\#T} \sum_{t \in T} \sum_{i=-\frac{v}{2}}^{\frac{v}{2}} w_i \sqrt[4]{a_{t;c_j+i}},$$

where $a_{t;k}$ denotes the amplitude of Fourier frequency k at time t, T is the set of all $\#T$ time-points periodograms are computed for, v is a pre-defined even bandwidth parameter and $w_i := \frac{2v-4|i|}{v^2}$ are linear weights as illustrated in Fig. 6 (b).

The aim underlying the construction of m is to prefer a choice of k_{supp} and k_{seal} which leads to BEFs meeting the area of high amplitudes as well as possible. The amplitudes are transformed as a consequence of the fact that the periodogram ordinates of White Noise are χ^2-distributed (see Theis (2003)). In this case by taking the 4^{th} root a symmetric distribution is obtained.

4 Results

Figure 7 shows an example fit after maximizing m by the optimization method of Nelder and Mead (1965). The technical settings are the same as in the previous section, $v = 50$ was chosen for the bandwidth. Some experiments with different choices of v between 15 and 100 showed that this parameter seems not to affect the results.

The optimal parameters are $\hat{k}_{supp} = 2.252 \cdot 10^8 \text{N/m}$ and $\hat{k}_{seal} = 1.037 \cdot 10^7 \text{N/m}$. The levels of these values are plausible from a technical point of view. Also their relation to each other is as expected since the damper is known to have a much higher stiffness influence than the seal.

Especially the higher third BEF fits the spectrogram quite well. A little bit different is the situation for the second one. Here the computed course seems to border the lower area of high amplitudes from above. The reason for the apparently unfavorable fit of the lower course of BEFs could be a the non-consideration of an important parameter. For example in some of our experiments we observed that the damper left its initial position d during the process. Since d is a very sensitive parameter in our model its time-variety should be taken into account in further investigations. Anyway we consider our assumption of seeing the bending eigenfrequencies in the acceleration signal confirmed.

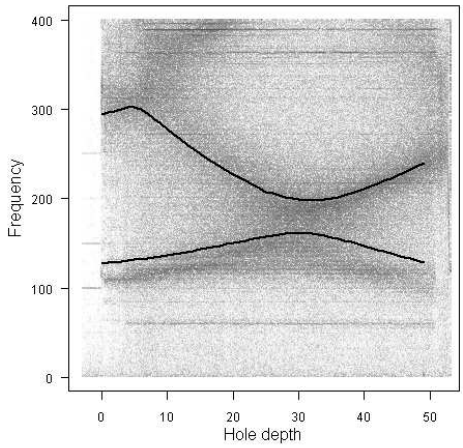

Figure 7: Fitted bending eigenfrequency courses.

5 Summary and Outlook

By the discretized analogous model we established a connection between measured data and the mechanics of the BTA system. The stiffness influences of the damper and the oil-supply-device have been identified to be the most important factors. Although further improvements are possible, we think the signal of the acceleration sensor is appropriate to estimate the time-variation of the BEFs.

One item of future work will be the consideration of further parameters like a variable damper or the implementation of a frequency response function. Improvements are also possible for the estimation procedure by taking the distribution of the periodograms into account.

The main goal of our investigations is the prevention of spiralling. So once the estimation of the BEFs is established, the next step will be online-estimation and connected to it the implementation of control charts. Then, when one BEF runs into danger to meet the rotational frequency or one of its uneven multiples, it maybe varied to avoid the intersection.

Acknowledgment

This work has been supported by the Collaborative Research Center 'Reduction of Complexity in Multivariate Data Structures' (SFB 475) of the

German Research Foundation (DFG).

References

GESSESSE, Y.B., LATINOVIC, V.N., and OSMAN, M.O.M. (1994): On the problem of spiralling in BTA deep-hole machining. *Transaction of the ASME, Journal of Engineering for Industry, 116*, 161–165.

GROSS, D., HAUGER, W., and SCHNELL, W. (2002a): *Technische Mechanik Band 3: Kinetik*, 7. ed., Springer, Berlin.

GROSS, D., HAUGER, W., SCHNELL, W. , and WRIGGERS, P. (2002b): *Technische Mechanik Band 4: Hydromechanik, Elemente der hheren Mechanik, Numerische Methoden*, 4. ed., Springer, Berlin.

NELDER, J.A. and MEAD, R. (1965): A Simplex Method for Functional Minimization. *Computer Journal, 7:308–313.*

RAABE, N., THEIS, W., and WEBBER, O. (2004): Spiralling in BTA Deep-Hole Drilling - How to model varying frequencies. *Conference CD of the Fourth Annual Meeting of ENBIS 2004*, Copenhagen.

THEIS, W. (2004): *Modelling Varying Amplitudes*, Dissertation, Fachbereich Statistik, Universität Dortmund, http://eldorado.uni-dortmund.de:8080/FB5/ls7/forschung/2004/Theis

VDI (1974): Tiefbohrverfahren. *VDI Düsseldorf.*